Cancer Chemotherapy and Pharmacology (2019) 84:527–537
https://doi.org/10.1007/s00280-019-03846-x

ORIGINAL ARTICLE

In vitro evaluation of FL118 and 9-Q20 cytotoxicity and cellular uptake in 2D and 3D different cell models

Qi Weng[1] · Leilei Zhou[2] · Lihua Xia[1] · Yixin Zheng[1] · Xiangli Zhang[1] · Fengzhi Li[3] · Qingyong Li[1,2]

Received: 21 January 2019 / Accepted: 22 April 2019 / Published online: 27 April 2019

Abstract

Purpose Recent researches are attempting to verify that the 3D cell models can provide a gap bridge between in vitro and in vivo for anticancer drug evaluations. The aim of this study was to continue the development of novel in vitro 3D cell models and the investigation of the cellular uptake mechanism of camptothecin (CPT) and its derivatives [FL118 (10,11-methylenedioxy-20(*S*)-camptothecin), 9-Q20 (9-*p*-trifluoromethylphenyl-10,11-methylenedioxy-20(*S*)-camptothecin)] in 2D and 3D cell models.

Methods The 3D cell models were established using ultralow attachment 96-well plates. The cytotoxicity of CPT, FL118, and 9-Q20 was evaluated by MTT method. The effects of compound concentration, incubation time, temperature, and transporter inhibitors on the cellular uptake of CPT, FL118, and 9-Q20 were examined in 2D and 3D cell models.

Results The cytotoxicity of CPT, FL118, and 9-Q20 was lower in 3D cell models than 2D cell models. In 2D Caco-2 cell model, the uptake rate of CPT, FL118, and 9-Q20 was faster during the early time of incubation. In 3D Caco-2 cell model, the uptake capacity of CPT, FL118, and 9-Q20 was significantly improved over time. In 3D Caco-2 cell model, Verapamil (P-gp inhibitor) and Gefitinib (BCRP inhibitor) more significantly increased the uptake of CPT and 9-Q20. In contrast, P-gp and BCRP did not affect the accumulation of FL118 in 2D and 3D Caco-2 cell models. The accumulation of CPT, FL118, and 9-Q20 was greater in HepG2 cells than HCT116 cells.

Conclusion The 3D cell models provided more potency information on the process of cellular uptake of CPT, FL118, and 9-Q20, which more objectively reflected the drug sensitivity and drug resistance in vivo compared with the 2D cell models.

Keywords FL118 · 9-Q20 · 3D culture · Ultralow attachment · Cytotoxicity · Cellular uptake

Abbreviations

3D	Three-dimensional
CPT	Camptothecin
FL118	10,11-Methylenedioxy-20(*S*)-camptothecin
9-Q20	9-*p*-Trifluoromethylphenyl-10,11-methylenedioxy-20(*S*)-camptothecin
2D	Two-dimensional
ULA	Ultralow attachment
P-gp	P-glycoprotein
BCRP	Breast cancer-resistance protein
HD	Hanging drop
Vp	Verapamil
LRP	Lung-resistance-related protein
GST-π	Glutathione-*S*-transfers-π
MRP1	Multidrug-resistance proteins-1

✉ Qingyong Li
liqy@zjut.edu.cn

[1] College of Pharmaceutical Science, Zhejiang University of Technology, No. 18 Chaowang Road, Hangzhou 310014, China

[2] Collaborative Innovation Center of Yangtze River Region Green Pharmaceuticals, Zhejiang University of Technology, Hangzhou, China

[3] Department of Pharmacology and Therapeutics, Roswell Park Comprehensive Cancer Center, Buffalo, NY, USA

Introduction

Cell-based assays have been widely used in preclinical anticancer drug discovery. In vitro cell-culture models are convenient and time-saving in discovering drug candidate molecules [1]. Over the past decade, cell models have been widely adopted as a drug-screening tool, including Caco-2 cell model, MDCK cell model, and MDR1–MDCK cell model [2, 3]. However, the 2D cellular micro-environment is different from in vivo conditions, which suffers

disadvantages concerning the lack of the micro-architecture, cell–cell, and cell–matrix interactions, thus leading to the therapy failure during in vivo trials [4]. Therefore, there is an urgent need to develop new cell models, which are capable of providing close predictions of drug efficacy in vivo.

In recent years, three-dimensional (3D) in vitro cell-culture models have been receiving increased attention for their applications in screening novel anticancer drugs [5, 6]. A variety of methods have been adopted to form 3D cell spheroids, including ultralow attachment (ULA) plates, hanging drop (HD) plates, microgravity bioreactor, and hydrogen-based matrices or solid scaffolds [1]. It has been well recognized that the 3D cell-culture models compensate for many defects that occur in 2D cell culture. For instance, cellular spheroids can develop gradients of oxygen, nutrients, metabolites, and soluble signals, thus creating heterogeneous cells population [7, 8]. Spheroids express cytokines, cell-signaling molecules, and drug responses in levels that resemble the in vivo conditions [9]. These features of the 3D cell-culture systems allow them to be applied to different studies, such as better drug-screening assays, pharmacological applications, gene and protein expression studies and the complex cellular physiological mechanisms, etc. [10–12]. Thus, we used 2D cell models versus 3D cell models to study the cytotoxicity and the uptake of drugs for evaluating the advantage of 3D over 2D cell models in this paper.

Camptothecin (CPT) has been shown potent antitumor activity, but its clinical utility was limited due to its poor water solubility, low bioavailability, and severe toxic side effects [13, 14]. Therefore, efficient and low-toxic CPT derivatives have been investigated in the past as well as in recent years. Irinotecan and topotecan, the water-soluble derivatives of CPT, have been approved by the FDA for cancer treatment in the clinic, which showed superior antitumor activity and less toxicity than CPT [15–17]. However, treatment resistance to irinotecan and topotecan is often observed in the clinical trials, especially in patients taking these drugs for a long period of time [18]. In 2012, using the survivin gene as a target and bio-marker in high-throughput screening of small molecule libraries, a novel CPT analogue, designated FL118, which is 10, 11-methylenedioxy-20(*S*)-camptothecin was re-discovered [19, 20]. In vitro and in vivo studies revealed that the antitumor efficacy of FL118 was superior to irinotecan, topotecan, doxorubicin, 5-FU, gemcitabine, docetaxel, oxaliplatin, cytoxan, and cisplatin [19, 21]. Moreover, FL118 showed superior antitumor, as it selectively inhibits survivin, Mcl-1, XIAP, and cIAP2 in a p53-independent manner rather than Topo I, which is different from other CPT derivatives [19]. FL118 is not a substrate of the efflux pump proteins BCRP and P-gp, so it can eliminate human tumors that acquire irinotecan and topotecan resistance [21, 22]. However, FL118 showed poor solubility in both the organic phase and the aqueous phase without special formulation [23]. Hence, it is important to increase its solubility and bioavailability not only by changing the formulation, but also by structural modification. We have synthesized a series of 9-substituted FL118 analogs by structural modification. Therefore, it is prospective work to further explore the antitumor activity and the cellular uptake of FL118 and its 9-substituted derivatives.

The main purpose of this study was to develop in vitro 3D cell models for evaluating the uptake of CPT, FL118, and 9-Q20 (9-*p*-trifluoromethylphenyl-10,11-methylenedioxy-20(*S*)-camptothecin). The drug absorption plays a key role in its efficacy, so the effects of compound concentration, incubation time, temperature, and transporter inhibitors on cellular uptake were studied in 2D versus 3D cell models. We also compared the anti-proliferation activity of CPT, FL118, and 9-Q20 against HCT116, MCF-7, HepG2, HeLa, and A549 cell lines using MTT assay.

Materials and methods

Chemicals and materials

DMEM was purchased from Gibco BRL Life Technology. DMSO, FBS was purchased from Hyclone. Hanks buffered salt solution (HBSS), phosphate-buffered saline (PBS), 100 U/mL of penicillin, and 100 µg/mL of streptomycin were purchased from Genom. 0.25% trypsin–EDTA, 0.4% Trypan and MTT were purchased from Solarbio. All reagents for HPLC were of analytical grade. CPT, Verapamil (Vp) and Gefitinib were purchased from Aladdin. FL118 and 9-Q20 (purity > 98%) were synthesized by our lab.

The blood-counting chamber was purchased from QIU JING® (Shanghai). 6-Well cell-culture plates, ULA 6-well flat-bottom plates, ULA 96-well flat-bottom plates, 96-well cell-culture plates, and T-25 cm^2 cell-culture flask were purchased from Costar® (Corning Incorporated, USA).

Cell line and culture conditions

Human colon cancer cells (HCT116), human breast cancer cells (MCF-7), human liver cancer cells (HepG2), human cervical cancer cells (HeLa), human alveolar basal epithelial cell-derived lung cancer cells (A549), and human colorectal cancer cells (Caco-2) were purchased from the China Center for Type Culture Collection (Wuhan, China). Cells were cultured in DMEM with 10% (v/v) FBS, 1% (v/v) penicillin and streptomycin in a humidified atmosphere containing 5% CO_2 at 37 °C.

Development and characterization of 3D Caco-2 spheroids

3D Caco-2 spheroids were generated using ULA 96-well flat-bottom plates. First, cell suspension was generated from trypsinized monolayer cells and diluted to the desired cell density (0.10×10^5, 0.50×10^5, 1.25×10^5, 2.50×10^5, and 5.00×10^5 cells/mL); then, 200 µL of cell suspension was added to each well in the ULA plates. After 24 h, 48 h, 72 h, 96 h, and 120 h, the changes in the diameter of spheroids were observed with a fluorescence microscope (Eclipse TS100, NIKON).

Cell viability assay

The anti-proliferation activity of CPT, FL118, and 9-Q20 against HCT116, MCF-7, HepG2, HeLa, A549, and Caco-2 cell lines was initially evaluated by MTT assay [24]. The cells were treated with compounds for 8 h or 72 h. The absorbance was measured at 570 nm using an ELISA Plate Reader (infinite M200 Pro, TECAN), and the background was subtracted at 630 nm. In each MTT assay, every group consisted of three replicates.

The Trypan Blue assay [25] was used to analyze the viability of 3D Caco-2 spheroids. The spheroids were dissociated using the trypsin–EDTA solution for 15 min. The cells were centrifuged, and then, HBSS solution was added. The cell suspension was mixed with 0.4% Trypan Blue (1: 9, v/v) and stained for 3–5 min. The number of cells in each well was estimated in triplicate using a blood-counting chamber under an inverted microscope. All experiments were performed in triplicate.

HPLC analysis

Samples were directly applied to HPLC analysis, performed on a Shimadzu HPLC system equipped with LC solution software, LC-20AT binary gradient pump, a CTO-10AS column oven, and an SPD-20A UV/Vis detector (Shimadzu, Kyoto, Japan). The HPLC separation was performed on a C18 (250 mm × 4.6 mm, 5 µm, Elite, Dalian) reverse-phase column maintained at 40 °C. The mobile phase of CPT and FL118 consisted of 0.1% formic acid and acetonitrile (60:40, v/v) with a 1.0 mL/min flow rate. The mobile phase of 9-Q20 consisted of 0.1% formic acid and acetonitrile (35:65, v/v) with a 1.0 mL/min flow rate. The absorbance detector wavelength was set at 360 nm, and the injection volume was 20 µL. The retention times of CPT, FL118, and 9-Q20 were 6.447 (Fig. 1a), 6.604 (Fig. 1b), and 6.783 min (Fig. 1c), respectively. Calibration curves were constructed over the concentration ranges 0.03–1.00 µM. Linear regression analysis of the peak area and concentration revealed a typical equation $y=9173x+228.68$ ($R^2=0.9992$) for CPT, a typical equation $y=10506x-41.154$ ($R^2=0.9995$) for FL118, and a typical equation $y=10025x-138.45$ ($R^2=0.9994$) for 9-Q20. The standard curves showed good linearity.

Cellular uptake in 2D and 3D cell models

Cell culture

When cells in the T-25 cm^2 cell-culture flask reached 80–90% confluence, the cells were digested with trypsin–EDTA to make cell suspension. 2 mL of cell suspension with a density of 2.50×10^5 cells/mL was seeded into each well of six-well plates and ULA six-well plates. Then, the plates were placed in a 37 °C, 5% CO_2 incubator for 3 days.

Cellular uptake kinetic

In 2D and 3D cell models, the effects of compound concentration, incubation time, temperature, and transporter inhibitors on cellular uptake of CPT, FL118, and 9-Q20

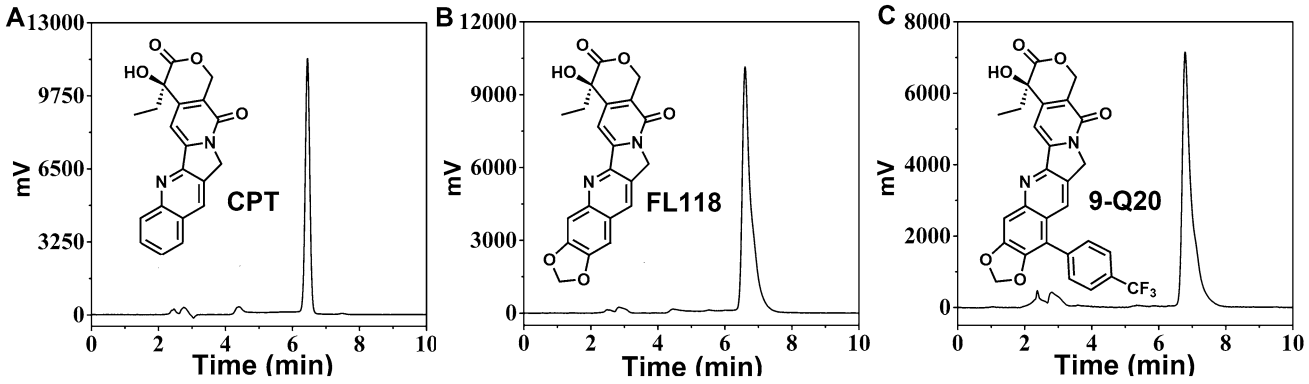

Fig. 1 Representative chromatograph: **a** CPT with retention time of 6.447 min, **b** FL118 with retention time of 6.604 min, **c** 9-Q20 with retention time of 6.783 min

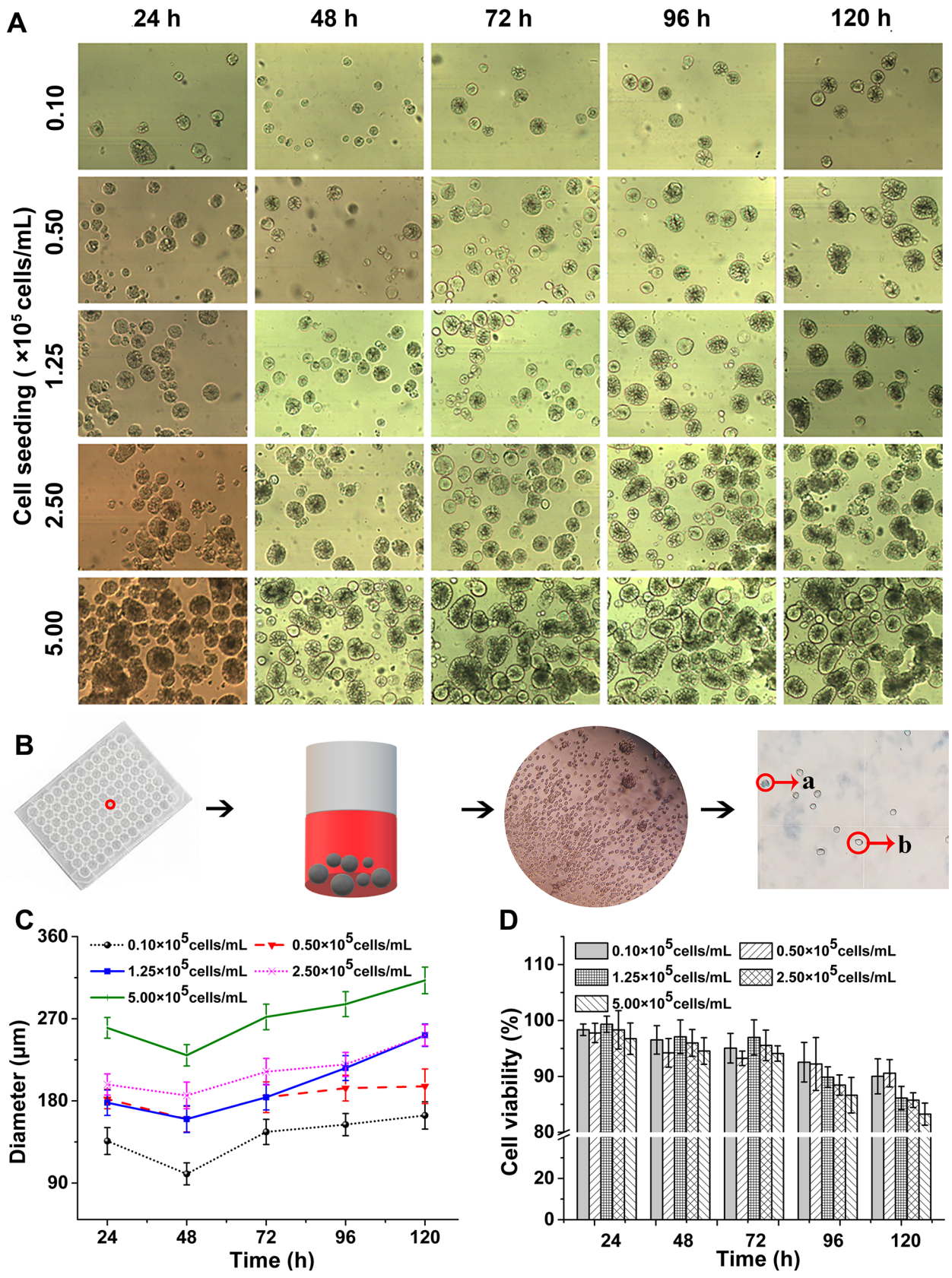
A
24 h
48 h
72 h
96 h
120 h
Cell seeding (×10^5 cells/mL)
0.10
0.50
1.25
2.50
5.00
B
a
b
C
0.10×10^5cells/mL
0.50×10^5cells/mL
1.25×10^5cells/mL
2.50×10^5cells/mL
5.00×10^5cells/mL
Diameter (μm)
360
270
180
90
24
48
72
96
120
Time (h)
D
0.10×10^5cells/mL
0.50×10^5cells/mL
1.25×10^5cells/mL
2.50×10^5cells/mL
5.00×10^5cells/mL
Cell viability (%)
110
100
90
80
20
0
24
48
72
96
120
Time (h)

◂**Fig. 2** **a** Fluorescence microscopic images of 5-day Caco-2 spheroids cultured in ULA 96-well flat-bottom plates with different cell-seeding concentrations (×4 objectives). **b** 3D Caco-2 spheroids were generated by ULA 96-well flat-bottom plates, which were dissociated by the trypsin–EDTA, then stained with TB. The number of cells in each well was estimated in triplicate using a blood-counting chamber under an inverted microscope (×10 objectives). The dead cells were dyed light blue (**a**), and the living cells were rejected (**b**). **c** Diameter of 3D Caco-2 spheroids was obtained using Image J software. **d** Viability of 3D Caco-2 spheroids. Curves represented triplicate biological repeats and were displayed as mean ± SD ($n = 3$)

were examined. In addition, the uptake of CPT, FL118, and 9-Q20 by different cell lines (Caco-2, HCT116, and HepG2) in 2D and 3D culture conditions was also investigated. The cells were cultured in cell-culture plates as described "Cell culture". Prior to administration, the cells were carefully washed three times with HBSS (pH 7.4) buffer. To optimize incubation time, the cells were incubated with CPT, FL118, and 9-Q20 (0.1, 0.3, 0.6, 0.8, or 1 μM) for 2, 4, or 8 h at 37 °C. To study the effects of compound concentration and temperature on the uptake of the compounds, the cells were exposed to the CPT, FL118, and 9-Q20 (0.1, 0.3, 0.6, 0.8, or 1 μM) for 4 h at 4 °C or 37 °C. To investigate the effect of transporter inhibitors on the uptake of the compound, after being pretreated with Vp (P-gp inhibitor, 1 μM) or Gefitinib (BCRP inhibitor, 1 μM) for 30 min [26], the cells were then incubated with CPT, FL118, and 9-Q20 (0.1, 0.3, 0.6, 0.8, or 1 μM) for 4 h at 37 °C.

At the prescribed timepoint, the plates were removed and placed on ice and washed three times with 4 °C HBSS. The 2D cells and 3D cells were digested with 200 μL of trypsin separately. The cell suspension was centrifuged at 5000 rpm for 10 min at 4 °C. The cells were washed three times with HBSS (pH 7.4) buffer, and then, 250 μL of HBSS buffer was added. After freeze-thawed three times at − 20 °C and then 40 °C, the solution was centrifuged at 10,000 rpm for 10 min. The supernatant was taken to determine the content of intracellular compound and protein.

Determination of compound and protein content

After centrifugation, 200 μL of the supernatant was taken and an equal volume of acetonitrile was added to cause denaturation of the protein and centrifuged for 10 min. The supernatant was aspirated, filtered through a 0.45 μm filter, and the content of intracellular compound was determined by HPLC. In this experiment, the total protein content in the cells was determined according to the Coomassie brilliant blue method [27]. The intracellular uptake of compound was expressed as the ratio of the intracellular compound content to the total intracellular protein content in nmol/mg protein.

Data analysis

Statistical and graphical information was determined using Origin® 9 software (Data Analysis and Graphing Software Incorporated). The results were reported as the mean ± standard deviation (SD). Differences between samples were analyzed using the Student's test. A p value of < 0.05 was considered statistically significant.

Results

Development and characterization of 3D Caco-2 spheroids

To generate spheroids for the uptake experiments, Caco-2 cells with a density of $0.10–5.00 \times 10^5$ cells/mL were seeded to the ULA 96-well plates and then incubated for 24 h, 48 h, 72 h, 96 h, and 120 h (Fig. 2a). The diameter of 3D Caco-2 spheroids was measured, and the viability of the 3D Caco-2 spheroids was evaluated by the Trypan Blue assay (Fig. 2b). As shown in Fig. 2c, a decrease on the size of the cell aggregates was observed, which became more compact, forming solid spheroids after 48 h. Furthermore, the viability of spheroids seeded with a low density of $0.10–0.5 \times 10^5$ cells/mL was maintained over 90% during the tested period of culture (Fig. 2d). In contrast, the viability of spheroids seeded with a high density of $1.25–5.00 \times 10^5$ cells/mL was maintained near 90% only during the first 72 h. Since the critical passive diffusion distance is 100 μm, spheroid size of more than 200 μm was used to determine the permeability [28]. The results showed that the size of spheroids seeded with a density of $2.50–5.00 \times 10^5$ cells/mL was larger than 200 μm after 72 h. Furthermore, the spheroids seeded with a density of 2.5×10^5 cells/mL presented round-type morphology well at 72 h. These observations indicated that the seeding density at 2.50×10^5 cells/mL and the 72 h culture time were the optimized culture conditions obtained for spheroids formation.

Differential cytotoxicity of 2D versus 3D cells up on compound treatment

The anti-proliferation activity of CPT, FL118, and 9-Q20 against HCT116, MCF-7, HepG2, HeLa, and A549 cell lines was evaluated by MTT assay. Table 1 shows that FL118 could effectively inhibit cancer cell growth at nM levels, which was consistent with the previous reports [19]. CPT, FL118, and 9-Q20 both had superior anti-proliferative effect on HCT116, MCF-7, and A549 cells than HepG2 cells. The 72 h MTT assay indicated that the antitumor activity of FL118 was superior to CPT. Camptothecins are effective in the treatment of advanced colon cancer and primary liver

Table 1 Mean (±SD) IC_{50} values (μM) of CPT, FL118, and 9-Q20 against the five tumor cell lines

Compound	Cell lines				
	HCT116	MCF-7	HepG2	HeLa	A549
CPT	0.14 ± 0.06	0.57 ± 0.03	1.39 ± 0.22	2.07 ± 0.31	0.17 ± 0.08
FL118	0.04 ± 0.01	0.03 ± 0.02	0.13 ± 0.02	0.03 ± 0.01	0.05 ± 0.03
9-Q20	0.93 ± 0.02	0.78 ± 0.02	3.58 ± 0.21	1.42 ± 0.11	0.80 ± 0.05

cancer in clinic [29, 30]. Therefore, not only the uptake of CPT, FL118, and 9-Q20 in 2D and 3D Caco-2 cell models was investigated, but also the relationship between the antiproliferation activity of the compound and its accumulation in HCT116 and HepG2 cell models.

To ensure that the compound concentration was nontoxic to the cells in the uptake test, it was necessary to determine the compound concentration and incubation time in the uptake test by the viability of the cells assay. The cytotoxicity of CPT, FL118, and 9-Q20 was evaluated by MTT assay in 2D and 3D cell models (Caco-2, HCT116, and HepG2). The cells were treated with CPT, FL118, and 9-Q20 (0.1, 0.3, 0.6, 0.8, or 1 μM) for 8 h. It was said that the cell viability more than 90% indicated that the tested compound concentration was almost nontoxic to the cells [24]. As shown in Fig. 3, no significant cytotoxicity of CPT, FL118, and 9-Q20 was observed

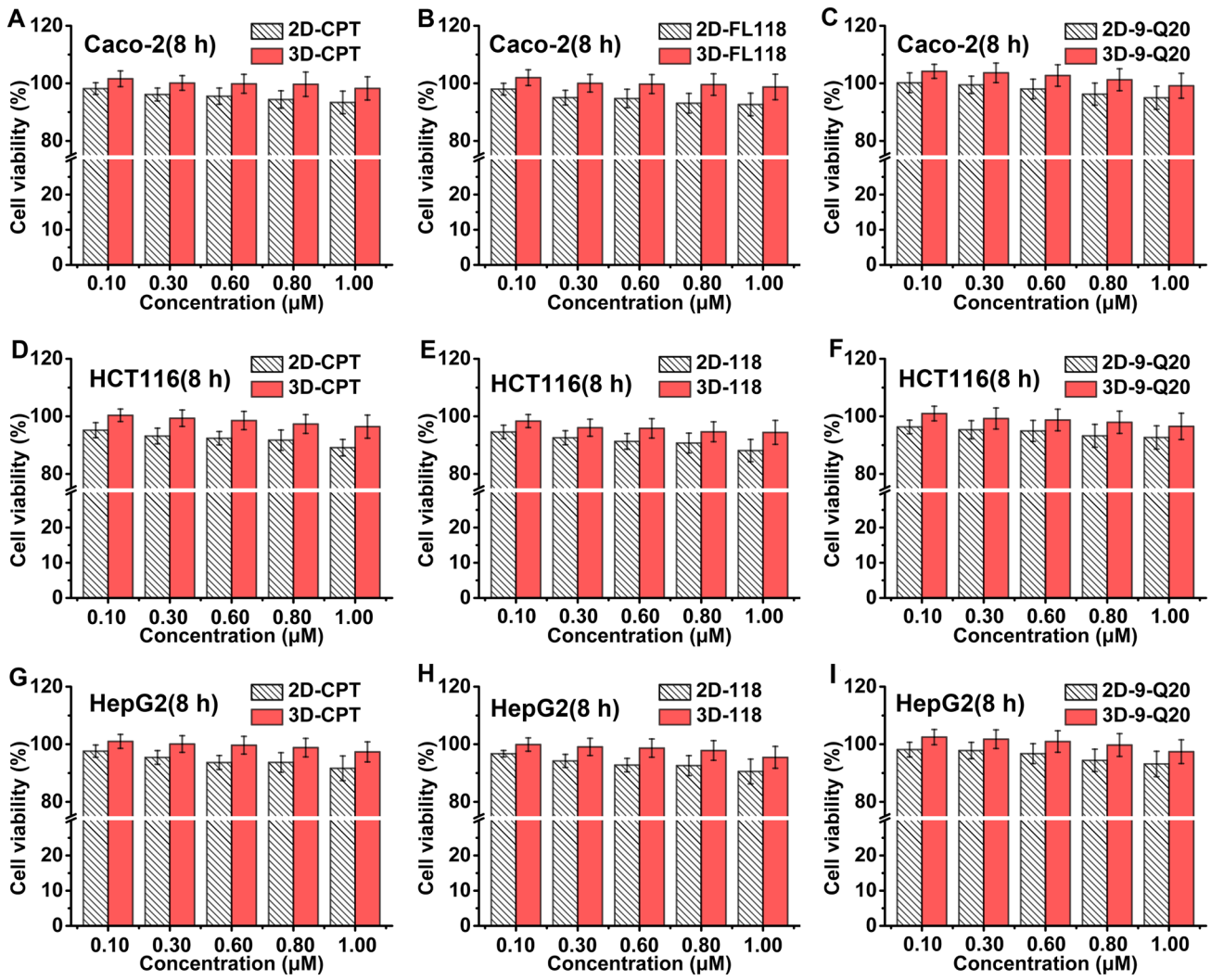

Fig. 3 Cytotoxicity of CPT, FL118, and 9-Q20 against Caco-2 (**a**–**c**), HCT116 (**d**–**f**) and HepG2 (**g**–**i**) cells in 2D and 3D culture conditions for 8 h. Data represented the mean ± SD from three replicate

in 2D and 3D cell models, and the cytotoxicity of CPT, FL118, and 9-Q20 was lower in 3D cell models.

Cellular uptake of CPT, FL118, and 9-Q20 in 2D and 3D cell models

Differential compound uptake in 2D versus 3D cell models over time

To investigate the effects of incubation time and the compound concentration on the uptake of CPT, FL118, and 9-Q20 in 2D and 3D Caco-2 cell models, cells were incubated with CPT, FL118, and 9-Q20 (0.1, 0.3, 0.6, 0.8, or 1 μM) for 2 h, 4 h, or 8 h at 37 °C. The results in Fig. 4a–f indicated the uptake of CPT, FL118, and 9-Q20 in 2D and 3D Caco-2 cell models was time and concentration dependent. In addition, the uptake of CPT, FL118, and 9-Q20 was greater in 2D Caco-2 cell model than 3D Caco-2 cell model (Fig. 4a–c). In addition, the uptake of 9-Q20 was the greatest among the tested compounds (Fig. 4c). In 3D Caco-2 cell model, the uptake capacity of CPT, FL118, and 9-Q20 was significantly improved at 4 h and 8 h (Fig. 4d–f). Thus, 4 h was selected as the incubation time in the following.

Differential compound uptake in 2D versus 3D cell models under different temperature

To determine the effect of temperature on the uptake of CPT, FL118, and 9-Q20 in 2D and 3D Caco-2 cell models, the cells were incubated with CPT, FL118, and 9-Q20 (0.1, 0.3, 0.6, 0.8, or 1 μM) at 37 °C or 4 °C for 4 h (Fig. 4g–i). Fig. 4h shows that the uptake of FL118 was similar at 4 °C and 37 °C in 2D and 3D Caco-2 cell models. It indicated that the absorption of FL118 in Caco-2 cells might depend on the passive diffusion. However, the uptake of CPT and 9-Q20 in 2D and 3D Caco-2 cell models was significantly increased at 4 °C (Fig. 4g, i), which suggested that the absorption of CPT and 9-Q20 in Caco-2 cells might depend not only on the passive diffusion, but also on the efflux pump-mediated process. Therefore, the effect of the efflux pump inhibitors on the cellular uptake of CPT, FL118, and 9-Q20 was further investigated in the following.

Differential effect of transporter inhibitors on the uptake of CPT, FL118, and 9-Q20

To investigate whether P-gp and BCRP transporter proteins mediate the uptake of CPT, FL118, and 9-Q20 in 2D and 3D cell models, the cells were pretreated with Vp or Gefitinib (1 μM) for 30 min and then incubated with CPT, FL118, and 9-Q20 (0.1, 0.3, 0.6, 0.8, or 1 μM) at 37 °C for 4 h (Fig. 5a–f.). Vp and Gefitinib increased the accumulation of CPT (Fig. 5a, d) and 9-Q20 (Fig. 5c, f) in 2D and 3D cell models. In addition, the uptake of CPT and 9-Q20 increased more significantly in 3D Caco-2 cell model. In contrast, Vp and Gefitinib did not affect the accumulation of FL118 in 2D and 3D Caco-2 cell models (Fig. 5b, e). This suggested that CPT and 9-Q20 were excreted via the efflux pump proteins P-gp and BCRP, whereas FL118 was not.

Differential compound uptake by different cell lines in 2D and 3D culture conditions

To study the uptake of CPT, FL118, and 9-Q20 by different cell lines in 2D and 3D culture conditions, HCT116 and HepG2 cells were incubated with CPT, FL118, and 9-Q20 (0.1, 0.3, 0.6, 0.8, or 1 μM) at 37 °C for 4 h (Fig. 5g–i). The accumulation of CPT, FL118, and 9-Q20 was greater in HepG2 cells than HCT116 cells. However, CPT, FL118, and 9-Q20 were more effective against HCT116 cells than HepG2 cells. Thus, the direct correlation between antitumor efficacy and the accumulation of compounds was not seen.

Discussion

Recently, 3D cell-culture systems have gained increasing interest in drug discovery due to their evident advantages in providing more physiologically relevant information and more predictive data for in vivo tests [31, 32]. The currently available methods of culturing 3D spheroids have met with shortcomings, such as lack of size control and difficulty in recovering spheroids from scaffolds [1]. In this study, ULA plates were used to form spheroids of uniform size quickly and easily, which made little well-to-well and plate-to-plate variation.

In this paper, 2D and 3D cell models were used to investigate the cytotoxicity and cellular uptake of CPT, FL118, and 9-Q20. The cytotoxicity of CPT, FL118, and 9-Q20 was lower in 3D cell models than 2D cell models. Compared with 2D monolayer cells, the 3D spheroids with increased cell–cell contact or tight packing might be hindering the drug penetration or diffusion into the spheroids [5]. The uptake rate of CPT, FL118, and 9-Q20 in 2D Caco-2 cell models was faster during the early time of incubation. However, the accumulation of CPT, FL118, and 9-Q20 in 2D and 3D Caco-2 cell models tended to approach after 8 h. The diffusion distance for the drug into the 2D monolayer cells was relatively short and easy, and its biological barriers were not adequately replicated in comparison with 3D spheroids [33]. In addition, the effect of temperature on the cellular uptake experiment showed that the absorption of CPT and 9-Q20 in Caco-2 cells might depend on not only the passive diffusion, but also the efflux pump-mediated process, but the absorption of FL118 in Caco-2 cells might only depend on the passive diffusion. Therefore, the effect of efflux pump

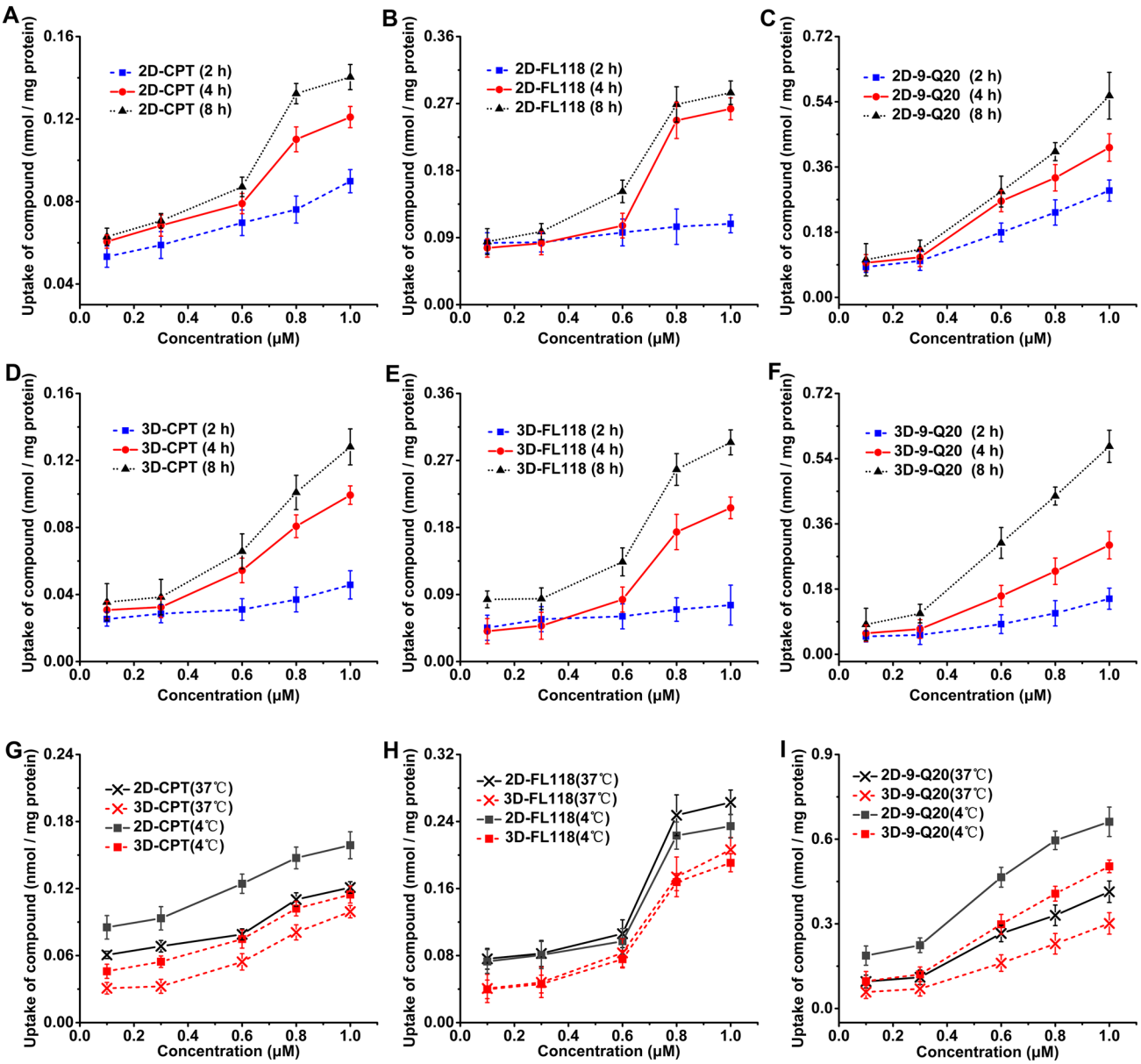

Fig. 4 Effects of time, compound concentration, and temperature on the uptake. The 2D and 3D Caco-2 cells were incubated with CPT, FL118, and 9-Q20 (0.1, 0.3, 0.6, 0.8, or 1 μM) for 2, 4, or 8 h at 37 °C (**a**–**f**). The 2D and 3D Caco-2 cells were exposed to the CPT, FL118, and 9-Q20 (0.1, 0.3, 0.6, 0.8, or 1 μM) for 4 h at 37 °C or 4 °C (**g**–**i**). Curves represented triplicate biological repeats and were displayed as mean ± SD ($n = 3$)

inhibitors on the cellular uptake of CPT, FL118, and 9-Q20 was further investigated.

Drug absorption is tightly controlled by biological barriers including the plasma membrane, transport proteins, and cellular efflux pumps [34, 35]. Efflux transporters, such as P-gp and BCRP, are well-known regulators of drug bioavailability, which can have profound pharmacological effects [36, 37]. It was reported that CPT and its derivatives (irinotecan and topotecan) were the substrates of P-gp and BCRP [13, 21, 22]. In this paper, the results showed that Vp and Gefitinib significantly increased the accumulation of CPT and 9-Q20 in 2D and 3D Caco-2 cell models, which indicated that the transport of CPT and 9-Q20 was mediated by P-gp and BCRP. In contrast, Vp and Gefitinib did not remarkably affect the accumulation of FL118 in 2D and 3D Caco-2 cell models, which was consistent with the previous reports that FL118 was not a substrate of P-gp and BCRP [20, 22]. The previous studies showed that the expression of several drug-resistance proteins, including lung-resistance-related protein (LRP), glutathione-S-transfers-π (GST-π),

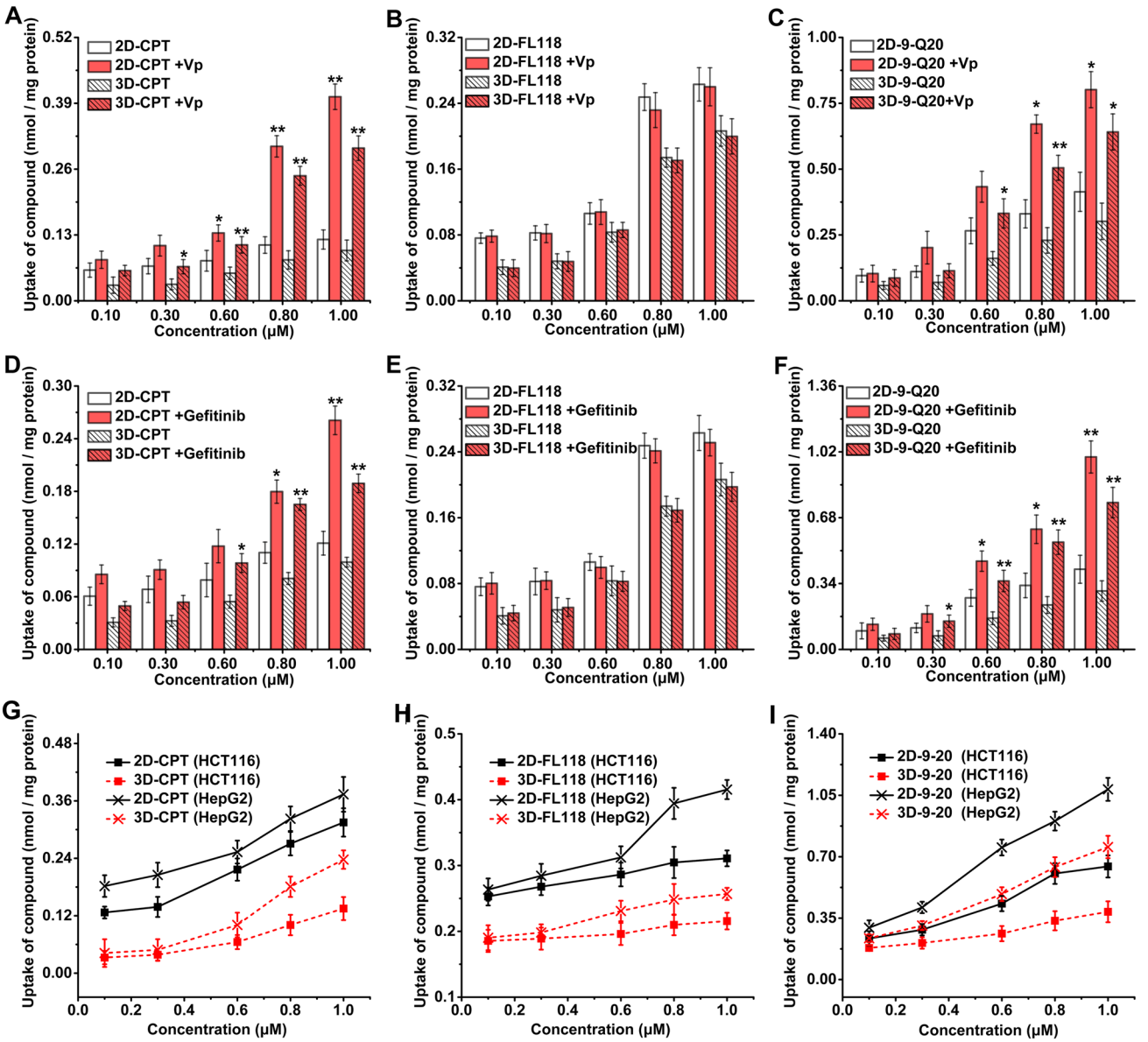

Fig. 5 Effect of transporter inhibitors on the uptake. The 2D and 3D Caco-2 cells were treated with or without Vp (1 μM) for 30 min and then exposed to CPT, FL118, and 9-Q20 (0.1, 0.3, 0.6, 0.8, or 1 μM) for 4 h at 37 °C (**a**–**c**). The 2D and 3D Caco-2 cells were treated with or without Gefitinib (1 mM) for 30 min and then exposed to CPT, FL118, and 9-Q20 (0.1, 0.3, 0.6, 0.8, or 1 μM) for 4 h at 37 °C (**d**–**f**). Data represented the mean ± SD from three replicates. *$p < 0.05$ represented significantly different from the control; **$p < 0.01$, represented more significantly different from the control. **g**–**i** Differential compound uptake by different cell lines HCT116 and HepG2 cells in 2D and 3D culture conditions was treated with CPT, FL118, and 9-Q20 (0.1, 0.3, 0.6, 0.8, or 1 μM) and incubated at 37 °C for 4 h. Curves represented triplicate biological repeats and were displayed as mean ± SD ($n = 3$)

and multidrug-resistance proteins-1 (MRP1), were all significantly enhanced in 3D cells [38]. Indeed, Vp and Gefitinib more significantly increased the uptake of CPT and 9-Q20 in 3D Caco-2 cell model. The results above confirmed that the 3D Caco-2 cell model is more suitable for observing the absorption of compounds.

The molecular structures might be related to the cellular uptake of CPT, 9-Q20, and FL118 in both 2D- and 3D-cell models. The previous studies focused on the CPT derivatives argue that highly lipophilic analogs provide several pharmaceutical advantages relative to water-soluble, such as lactone stability, lack of metabolic conversion, broad antitumor activity, oral bioavailability, and optimized therapeutic efficiency [39–42]. This study showed that the uptake of FL118 was greater than that of CPT. 9-Q20 is a derivative of FL118 with the 9-position substituted trifluoromethylphenyl, and its absorption was improved compared with raw FL118. However, it also increased the chance of binding to

efflux pump proteins, which might result in the decrease on the accumulation of 9-Q20 in vivo. Therefore, the substrate specificity of some transporters must be taken into account when the new candidates are designed.

All the results indicated that there were distinct differences between the 2D and 3D cell models. Since 3D cell spheroids properly mimic the complexity of the in vivo environment, they provide a better cell model system for drug penetration and offer a new opportunity for drug discovery and drug action [43]. Consequently, 3D cell models in vitro will be applied to predict drug sensitivity and drug resistance in vivo in the future, which can provide more accurate and abundant information of drug mechanism compared with 2D cell models.

Acknowledgements We thank Ms. Amanda Hess for editorial proofreading of the manuscript before submission. This work was financially supported by Qianjiang talents project in Zhejiang province.

Compliance with ethical standards

Conflict of interest We would like to submit the manuscript entitled "In vitro evaluation of FL118 and 9-Q20 cytotoxicity and cellular uptake in 2D and 3D different cell models" to be considered for publication in "Cancer Chemotherapy and Pharmacology" as an original research report. There is no conflict of interest in the submission of this manuscript, and I would like to declare on behalf of my co-authors that the work has not been published before, or under consideration for publication elsewhere in whole or in part. All the authors listed have approved the manuscript enclosed.

References

1. Fang Y, Eglen RM (2017) Three-dimensional cell cultures in drug discovery and development. SLAS Discov 22(5):456–472. https://doi.org/10.1177/1087057117696795
2. Huimin L, Ming H (2005) Absorption and metabolism of genistein and its five isoflavone analogs in the human intestinal Caco-2 model. Cancer Chemother Pharmacol 55(2):159–169
3. Chantal B, JérMe G, Michel D, Chantal F, Dominique B, Richard B (2005) Inhibition of P-glycoprotein transport function and reversion of MDR1 multidrug resistance by cnidiadin. Cancer Chemother Pharmacol 56(2):173–181
4. Ya C, Depinho RA, Matthias E, Karen V (2011) Cancer research: past, present and future. Nat Rev Cancer 11(10):749–754
5. Shin CS, Kwak B, Han B, Park K (2013) Development of an in vitro 3D tumor model to study therapeutic efficiency of an anticancer drug. Mol Pharm 10(6):2167–2175
6. Watanabe T, Hasegawa T, Takahashi H, Ishibashi T, Itagaki H, Sugibayashi K (2002) Utility of MTT assay in three-dimensional cultured human skin model as an alternative for draize skin irritation test: approach using diffusion law of irritant in skin and toxicokinetics–toxicodynamics correlation. Pharm Res 19(5):669–675
7. Jong Bin K (2005) Three-dimensional tissue culture models in cancer biology. Semin Cancer Biol 15(5):365–377
8. Krause S, Maffini MV, Soto AM, Sonnenschein C (2010) The microenvironment determines the breast cancer cells' phenotype: organization of MCF7 cells in 3D cultures. BMC Cancer 10(1):263–263
9. Chandraiah G, Mandip S (2016) AlgiMatrix?-based 3D cell culture system as an in vitro tumor model: an important tool in cancer research. Methods Mol Biol 1379:117–128
10. Chitrangi S, Nair P, Khanna A (2017) 3D engineered in vitro hepatospheroids for studying drug toxicity and metabolism. Toxicol In Vitro 38:8–18. https://doi.org/10.1016/j.tiv.2016.10.009
11. Bartusik D, Tomanek B, Siluk D, Kaliszan R (2010) 19F MRI of 3D CEM cells to study the effects of tocopherols and tocotrienols. J Pharm Biomed Anal 53(3):599–602. https://doi.org/10.1016/j.jpba.2010.04.009
12. Chitcholtan Kenny, Sykes Peter H, Asselin Eric, Sophie Evans (2013) Differences in growth properties of endometrial cancer in three; dimensional (3D) culture and 2D cell monolayer. Exp Cell Res 319(1):75–87
13. Lalloo AK, Luo FR, Guo A, Paranjpe PV, Lee S-H, Vyas V, Rubin E, Sinko PJ (2004) Membrane transport of camptothecin: facilitation by human P-glycoprotein (ABCB1) and multidrug resistance protein 2 (ABCC2). BMC Med 2(1):16. https://doi.org/10.1186/1741-7015-2-16
14. Gottlieb JA, Guarino AM, Call JB, Oliverio VT, Block JB (1970) Preliminary pharmacologic and clinical evaluation of camptothecin sodium (NSC-100880). Cancer Chemother Rep 54(6):461–470
15. Marzi L, Agama K, Murai J, Difilippantonio S, James A, Peer CJ, Figg WD, Beck D, Msa E, Cushman M (2018) Novel fluoroindenoisoquinoline non-camptothecin topoisomerase I inhibitors. Mol Cancer Ther 17(8):1694–1704
16. Masuda N, Kudoh S, Fukuoka M (1996) Irinotecan (CPT-11): pharmacology and clinical applications. Crit Rev Oncol Hematol 24(1):3–26. https://doi.org/10.1016/1040-8428(96)00201-6
17. Lorusso D, Pietragalla A, Mainenti S, Masciullo V, Di VG, Scambia G (2010) Review role of topotecan in gynaecological cancers: current indications and perspectives. Crit Rev Oncol Hematol 74(3):163–174
18. Biren S, Murugesan G, Jayeeta D, Ahamed S, Celeste C, Luz Z, Ahamed N, Mecide G, Dale S, Yong L (2008) Sequential topoisomerase targeting and analysis of mechanisms of resistance to topotecan in patients with acute myelogenous leukemia. Anticancer Drugs 19(4):411–420
19. Xiang L, Cao S, Cheng Q, Keefe JT, Rustum YM, Li F (2012) A novel small molecule FL118 that selectively inhibits survivin, Mcl-1, XIAP and cIAP2 in a p53-independent manner, shows superior antitumor activity. PloS One 7(9):e45571
20. Li F, Ling X, Harris DL, Liao J, Wang Y, Westover D, Jiang G, Xu B, Boland PM, Jin C (2017) Topoisomerase I (Top1): a major target of FL118 for its antitumor efficacy or mainly involved in its side effects of hematopoietic toxicity? Am J Cancer Res 7(2):370–382
21. Xiang L, Xiaojun L, Kai Z, Nicholas S, Joshua P, Fengzhi L (2015) FL118, a novel camptothecin analogue, overcomes irinotecan and topotecan resistance in human tumor xenograft models. Am J Transl Res 7(10):1765–1781
22. Westover D, Ling X, Lam H, Welch J, Jin C, Gongora C, Del Rio M, Wani M, Li F (2015) FL118, a novel camptothecin derivative, is insensitive to ABCG2 expression and shows improved efficacy in comparison with irinotecan in colon and lung cancer models with ABCG2-induced resistance. Mol Cancer 14(1):92. https://doi.org/10.1186/s12943-015-0362-9
23. Ling X, Li F (2013) An intravenous (i.v.) route-compatible formulation of FL118, a survivin, Mcl-1, XIAP, and cIAP2 selective inhibitor, improves FL118 antitumor efficacy and therapeutic index (TI). Am J Transl Res 5(2):139
24. Zhen Z, Shen ZL, Zhai S, Xu JL, Hui L, Qin S, Li QY (2017) Transport of curcumin derivatives in Caco-2 cell monolayers. Eur J Pharm Biopharm 117:123–131

25. Piccinini F, Tesei A, Arienti C, Bevilacqua A (2017) Cell counting and viability assessment of 2D and 3D Cell cultures: expected reliability of the Trypan Blue assay. Biol Proced Online 19(1):8
26. Curran S, Achilli TM, Leary E, Wilks BT, Vantangoli MM, Boekelheide K, Morgan JR (2015) A 3D spheroid system to evaluate inhibitors of the ABCG2 transporter in drug uptake and penetration. Technology 3(01):54–63
27. Liang QQ, Li YS (2013) A rapid and accurate method for determining protein content in dairy products based on asynchronous-injection alternating merging zone flow-injection spectrophotometry. Food Chem 141(3):2479–2485
28. Franziska H, Heike M, Claudia D, Jonathan W, Wolfgang MK, Kunz-Schughart LA (2010) Multicellular tumor spheroids: an underestimated tool is catching up again. J Biotechnol 148(1):3–15
29. JérMe A, Jean-Marie T, Marine GG, Jean-Marie G, Didier R, Daniel A, Jean-Louis M, FranOis G (2002) Combination of topotecan and oxaliplatin in inoperable hepatocellular cancer patients. Am J Clin Oncol 25(2):198
30. Tomoo S, Jun-Ichi T, Toshitaka F, Koji F, Koji K, Shuji M, Satoshi M, Akihiko G, Narikazu B (2013) risk factors for severe adverse effects and treatment-related deaths in japanese patients treated with irinotecan-based chemotherapy: a postmarketing survey. Jpn J Clin Oncol 43(5):483–491
31. Karlssona H, Larsson R, Nygren P (2012) Loss of cancer drug activity in colon cancer HCT-116 cells during spheroid formation in a new 3-D spheroid cell culture system. Exp Cell Res 318(13):1577–1585
32. Breslin S, O'Driscoll L (2013) Three-dimensional cell culture: the missing link in drug discovery. Drug Discov Today 18(5–6):240–249
33. Achilli TM, Mccalla S, Meyer J, Tripathi A, Morgan JR (2014) Multilayer spheroids to quantify drug uptake and diffusion in 3D. Mol Pharm 11(7):2071–2081
34. Jang SH, Wientjes MG, Lu D, Au JL-S (2003) Drug delivery and transport to solid tumors. Pharm Res 20(9):1337–1350. https://doi.org/10.1023/a:1025785505977
35. Elliott NT, Yuan F (2015) A review of three-dimensional in vitro tissue models for drug discovery and transport studies. J Pharm Sci 100(1):59–74
36. Szakács G, Váradi A, Özvegy-Laczka C, Sarkadi B (2008) The role of ABC transporters in drug absorption, distribution, metabolism, excretion and toxicity (ADME–Tox). Drug Discov Today 13(9):379–393
37. Huang SM (2010) Membrane transporters in drug development. Nat Rev Drug Discov 9(3):215–236
38. Sun FF, Hu YH, Xiong LP, Tu XY, Zhao JH, Chen SS, Song J, Ye XQ (2015) Enhanced expression of stem cell markers and drug resistance in sphere-forming non-small cell lung cancer cells. Int J Clin Exp Pathol 8(6):6287
39. Hans G, Ramon S, Jaap V, George P, Jonge MJA, De Martin D, Christel VH, Francis S, Rosendo O, Joan PO (2003) Phase I pharmacological and bioavailability study of oral diflomotecan (BN80915), a novel E-ring-modified camptothecin analogue in adults with solid tumors. Clin Cancer Res 9(11):4101–4107
40. Graziella P, Beretta GL, Franco Z (2004) Gimatecan, a novel camptothecin with a promising preclinical profile. Anticancer Drugs 15(6):545
41. Min H, Heyong G, Yi C, Hong Z, Yujun C, Xiongwen Z, Zehong M, Hualiang J, Jian Z, Hongwu S (2007) Chimmitecan, a novel 9-substituted camptothecin, with improved anticancer pharmacologic profiles in vitro and in vivo. Clin Cancer Res 13(4):1298–1307
42. Rodríguez-Berna G, Mangas-Sanjuán V, Gonzalez-Alvarez M, Gonzalez-Alvarez I, García-Giménez JL, Cabañas MJD, Bermejo M, Corma A (2014) A promising camptothecin derivative: semisynthesis, antitumor activity and intestinal permeability. Eur J Med Chem 83(16):366–373
43. Smalley K, Lioni M, Herlyn M (2006) Life isn't flat: taking cancer biology to the next dimension. Vitro Cell Dev Biol Anim 42(8/9):242–247